

## Chapter 21

# ESTIMATION OF REGIONAL ACTUAL EVAPOTRANSPIRATION IN THE PANAMA CANAL WATERSHED

Jan M.H. Hendrickx<sup>1</sup>, Wim G.M. Bastiaanssen<sup>2</sup>, Edwin J.M. Noordman<sup>2</sup>,  
Sung-Ho Hong<sup>1</sup>, and Lucas E. Calvo-Gobbetti<sup>3</sup>

<sup>1</sup>New Mexico Tech, <sup>2</sup>WaterWatch, <sup>3</sup>Universidad Tecnológica de Panama

**Abstract:** The upper Río Chagres basin is a part of the Panama Canal Watershed. The least known water balance component of this watershed is evapotranspiration. Measurements of actual evapotranspiration rates on the ground are difficult and expensive. The objective of this study is to demonstrate a new inexpensive method for determination of regional evapotranspiration in the watershed. The method uses LANDSAT satellite images that are analyzed using the Surface Energy Balance Algorithms for Land (*SEBAL*). We use an image from March 27, 2000, for estimation of the distribution of the regional actual evapotranspiration in the Panama Canal Watershed and surrounding areas.

**Key words:** Panama Canal Watershed; evapotranspiration; *SEBAL*; remote sensing

## 1. INTRODUCTION

The upper Río Chagres basin is a part of the greater Panama Canal Watershed (see Georgakakos and Sperflage, 2005, this volume, Fig. 1). The least known water balance component of this watershed is evapotranspiration. Measurements of actual evapotranspiration rates on the ground are difficult, expensive, and therefore not usually included in operational water budget analyses. The objective of this study is to demonstrate a new and inexpensive method for determination of regional actual evapotranspiration across a watershed. The method uses LANDSAT satellite images that are analyzed using the Surface Energy Balance Algorithms for Land (*SEBAL*). As an example of the *SEBAL* potential, a LANDSAT image for Panama from 27 March 2000 is used to estimate the

distribution of the regional actual evapotranspiration (ET) in the Panama Canal Watershed and surrounding areas.

## 2. SURFACE ENERGY BALANCE ALGORITHM FOR LAND (*SEBAL*)

### 2.1 Remote Sensing for Evapotranspiration

Remote sensing methods use surface reflectances and the radiometric surface temperature from satellite spectral measurements to estimate ET from local to regional scales. First, surface parameters such as albedo, surface temperature, and vegetation indices are derived for each image pixel. Next, these surface parameters, together with field data, are used to solve the energy balance and ET is taken as the residual term. Following partly Kustas and Norman (1996), four different groups of remote sensing methods are recognized: (i) statistical methods, (ii) numerical simulation models, (iii) land use maps combined with traditional ET equations, and (iv) physically-based analytical approaches. The statistical methods relate the difference between satellite observed surface temperature and air temperature to ET (*e.g.*, Jackson *et al.*, 1977; Nieuwenhuis *et al.*, 1985; Seguin and Itier, 1983). These approaches require few input data, but often assume all meteorological variables but surface temperature spatially constant. This limits their application to homogeneous regions. Numerical models solve the equations of the energy and mass flow processes in the soil-vegetation-atmosphere system (*e.g.*, Camillo *et al.*, 1983; Carlson *et al.*, 1994; Sellers *et al.*, 1992) and require many input variables describing soil and vegetation properties. Since such detailed data sets are rarely available on regional scales, these models are less suitable for many satellite remote sensing hydrology studies. Current methods to compute ET over the irrigated and riparian areas of river valleys and rangelands in the western United States use remote sensing and GIS tools to create land use maps. This information, together with standard meteorological measurements, becomes input into traditional ET equations. These procedures are often cumbersome, slow, and expensive to implement and can have large uncertainty.

Physically based analytical methods evaluate the components of the energy balance and generally determine the ET rate as the residual:

$$R_n + G + H = \lambda E \quad (1)$$

where  $R_n$  is the net incoming radiation flux density ( $\text{W/m}^2$ ),  $G$  is the ground heat flux density ( $\text{W/m}^2$ ),  $H$  is the sensible heat flux density ( $\text{W/m}^2$ ), and  $\lambda E$  is the latent heat flux density ( $\text{W/m}^2$ ), which is the ET rate. The parameter  $\lambda$  in Equation (1) is the latent heat of vaporization of water ( $\text{J/kg}$ ) and  $E$  is the vapor flux density ( $\text{kg/m}^2/\text{s}$ ). In many remote sensing evaporation algorithms evaporation  $E$  includes not only bare soil evaporation but also canopy transpiration. This notation is followed in this paper.

The main challenge in the energy balance is to determine the partitioning of the available energy ( $R_n - G$ ) into  $\lambda E$  and  $H$ . The net radiation  $R_n$  is estimated from the remotely sensed surface albedo, surface temperature, and solar radiation calculated from standard astronomical formulae (Iqbal, 1983). The ground heat flux  $G$  is determined through semi-empirical relationships with  $R_n$ , surface albedo, surface temperature, and vegetation index. The most critical factor in the physically based remote sensing algorithms is to solve the equation for the sensible heat:

$$H = \rho_a c_p \frac{T_{aero} - T_a}{r_{ah}} \quad (2)$$

where  $\rho_a$  is the density of air ( $\text{kg/m}^3$ ),  $c_p$  is the specific heat of air ( $\text{J/kg/K}$ ),  $r_{ah}$  is the aerodynamic resistance to heat transfer ( $\text{s/m}$ ),  $T_{aero}$  is the surface aerodynamic temperature, and  $T_a$  is the air temperature either measured at a standard screen height or the potential temperature in the mixed layer (Brutsaert *et al.*, 1993). The aerodynamic resistance to heat transfer is affected by windspeed, atmospheric stability, and surface roughness (Brutsaert, 1982). The simplicity of Equation (2) is quite deceptive since  $T_{aero}$  cannot be measured by remote sensing. Remote sensing techniques measure the radiometric surface temperature  $T_{rad}$ , which is not the same as the aerodynamic temperature. The two temperatures usually differ by 1 to  $5^\circ\text{C}$ . Unfortunately, a small uncertainty of  $1^\circ\text{C}$  in  $T_{aero} - T_a$  can result in a  $50 \text{ W/m}^2$  uncertainty in  $H$  (Campbell and Norman, 1998). Although many investigators have tried to solve this problem by adjusting  $r_{ah}$  or using an additional resistance term, no generally applicable method has been developed yet (Kustas and Norman, 1996). Therefore, Campbell and Norman (1998) conclude that a practical method for using satellite surface temperature measurements should have at least three qualities: (i) accommodate the difference between aerodynamic temperature and radiometric temperature, (ii) not require a measurement of near-surface air temperature, and (iii) rely more on differences of surface temperature over

time or space rather than absolute surface temperatures to minimize the influence of atmospheric corrections and uncertainties in surface emissivity.

## 2.2 The Surface Energy Balance Algorithm for Land (SEBAL) Method

*SEBAL* is a practical method that meets the three requirements formulated by Campbell and Norman (1998). It overcomes the problem of inferring the aerodynamic temperature from the radiometric temperature and the need for near-surface air temperature measurements by directly estimating the temperature difference between a  $T_1$  and a  $T_2$  taken at two arbitrary levels  $z_1$  and  $z_2$  without explicitly solving the absolute temperature at a given height. The temperature difference for a dry surface without evaporation is obtained from the inversion of the sensible heat transfer equation with latent heat flux  $\lambda E=0$  so that  $H=R_n-G$  (Bastiaanssen *et al.*, 1998a):

$$T_1 - T_2 = \Delta T_a = \frac{H r_{ah}}{\rho_a c_p} \quad (3)$$

For a wet surface all available energy  $R_n-G$  is used for evaporation  $\lambda E$  so that  $H=0$  and  $\Delta T_a=0$ . Field observations have indicated that land surfaces with a high  $\Delta T_a$  are associated with high radiometric temperatures and those with a low  $\Delta T_a$  with low radiometric temperatures. For example, in New Mexico and Idaho, moist irrigated fields have a much lower  $\Delta T_a$  than dry rangelands. Field measurements in Egypt and Niger (Bastiaanssen *et al.*, 1998b), China (Wang *et al.*, 1998), USA (Franks and Beven, 1997), and Kenya (Farah, 2001) have shown that the relationship between  $T_{rad}$  and  $\Delta T_a$  is linear, such that:

$$\Delta T_a = c_1 T_{rad} - c_2 \quad (4)$$

where  $c_1$  and  $c_2$  are the linear regression coefficients valid for one particular moment (the time and date the image is taken) and landscape. By using the minimum and maximum values of  $\Delta T_a$  as calculated for the coldest and warmest pixel(s), the extremes of  $H$  are used to find the regression coefficients  $c_1$  and  $c_2$  which will prevent outliers of  $H$ -fluxes. Thus, the empirical Equation (4) meets the third quality stated by Campbell and Norman (1998) that one should rely on differences of the radiometric surface temperature over space rather than absolute surface temperatures, to minimize the influence of atmospheric corrections and uncertainties in surface emissivity.

Equation (3) has two unknowns:  $\Delta T_a$  and the aerodynamic resistance to heat transfer  $r_{ah}$ , which is affected by wind speed, atmospheric stability, and surface roughness (Brutsaert, 1982). Several algorithms take a few field measurements of wind speed and consider these as spatially constant over representative parts of the landscape (e.g., Hall *et al.*, 1992; Kalman and Jupp, 1990; Rosema, 1990). This assumption is only valid for uniform homogeneous surfaces. For heterogeneous landscapes a wind speed near the ground surface is required for each pixel. One way to overcome this problem is to consider the wind speed spatially constant at a height of 200 m above ground level. This is a reasonable assumption since at this height the wind speed is not affected by local surface heterogeneities. The wind speed at this height is obtained by an upward extrapolation of one wind speed measurement at 2 or 10 m to 200 m using a logarithmic wind profile. The wind speed at each pixel is obtained by a downward extrapolation using the surface roughness, which is determined for each pixel using an empirical relationship between surface momentum roughness  $z_{0m}$  and the Normalized Difference Vegetation Index (NDVI) or the Soil Adjusted Vegetation Index - SAVI (Huette, 1988). The end result of all these calculations is the determination of a  $r_{ah}$  and  $\Delta T_a$  for each pixel which allows us to find the sensible heat flux for each pixel. After inserting  $R_n$ ,  $G$ , and  $H$  into Equation (1) the latent heat flux  $\lambda E$  or ET rate is derived for each pixel.

Is *SEBAL* 'old technology'? *SEBAL* has the three qualities that Campbell and Norman (1998) deem necessary for a practical method that uses satellite surface temperature measurements for determination of consumptive water use. At first sight *SEBAL* is quite similar to other ET methods that use  $T_{rad}$  and  $\Delta T$  but with one significant difference. *SEBAL* uses an internal auto-calibration process that eliminates the need for actual measurements of  $T_{rad}$  and/or  $\Delta T$  as well as for atmospheric corrections. *SEBAL* is automatically calibrated for biases through the regression calibration of Equation (4), which is based on a cold and warm pixel. Thus, the surface temperature  $T_{rad}$  is used as a distribution parameter for partition of the sensible and latent heat flux.  $\Delta T_a$  floats above the land surface as it is indexed to  $T_{rad}$ , through calibration Equation (4), but it does not require actual measurements on the ground or atmospheric corrections.

### 2.3 Daily Actual Evapotranspiration

*SEBAL* yields an estimate of the instantaneous ET (mm/hour) at the time of the LandSat overpass around 11:00 am. This hourly ET rate needs to be extrapolated to the daily ET. The extrapolation is done using the evaporative fraction (*i.e.*, the ratio of latent heat over the sum of latent and sensible heat)

that has been shown to be approximately constant during the day. Therefore, multiplication of the evaporative fraction determined from *SEBAL* with the total daily available energy yields the daily evapotranspiration rate.

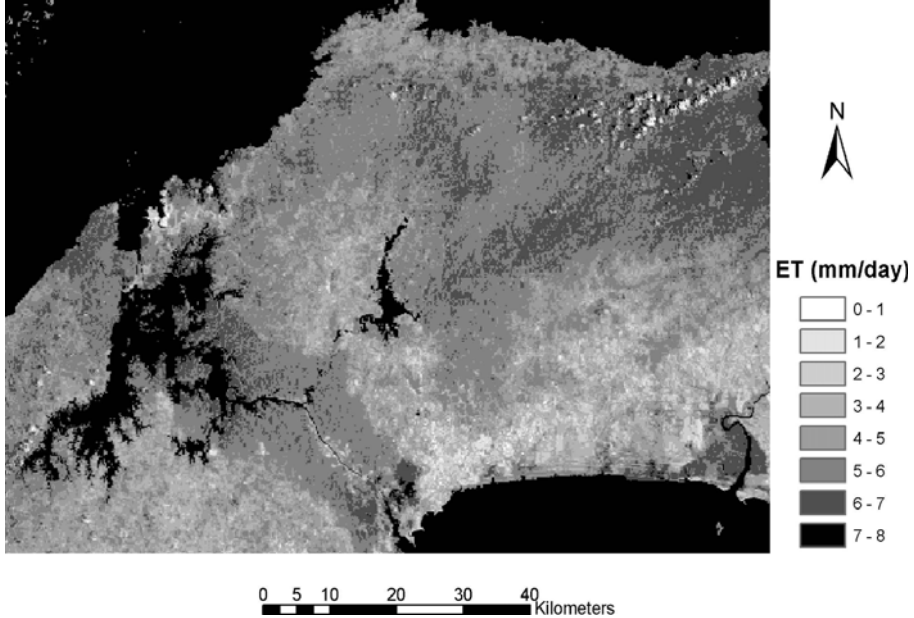


Figure 1. Daily actual evapotranspiration rates on 27 March 2000, in the Panama Canal Watershed and surrounding areas derived from *SEBAL*.

## 2.4 *SEBAL* Applications

*SEBAL* has only recently been validated (Bastiaanssen *et al.*, 1998a,b, 2002; Bastiaanssen, 2000) and appears rather insensitive for errors in parameters such as NDVI and atmospheric disturbances (Hendrickx *et al.*, 2002). *SEBAL* has matched latent heat flux measurements on the ground very well in Spain, Italy, Turkey, Pakistan, India, Sri Lanka, Egypt, Niger, and China (Bastiaanssen *et al.*, 1998a,b; Bastiaanssen and Bos, 1999; Bastiaanssen, 1995, 2000), Idaho (Allen *et al.*, 2001), and more recently New Mexico (Hendrickx, web site: [www.sahra.arizona.edu/research/TA2](http://www.sahra.arizona.edu/research/TA2)) and yields robust estimates of consumptive water use in large irrigated areas. Previous applications in the humid tropics of Sri Lanka and Kenya (Farah, 2001) confirm its potential for the Panama Canal Watershed.

### 3. THE APPLICATION OF *SEBAL* IN THE PANAMA CANAL WATERSHED

*SEBAL* has been applied to a LANDSAT image of 27 March 2000, which covers the entire Panama Canal Watershed, for determination of the regional actual evapotranspiration in the central Panama. The watershed includes lakes, tropical forests, agricultural lands, and bare soils. The evaporation rates vary from as high as 7 mm/day in the lakes to as low as 1 mm/day in urban areas. There is a striking difference between the undisturbed natural forest areas along the Canal and inside the upper Río Chagres watershed, with evaporation rates around 6 to 4 mm/day, and those of cleared lands used for agriculture, which exhibit rates around 4 to 2 mm/day. The deep-rooted trees have still access to sufficient root zone soil moisture to maintain a relatively high transpiration rate while the shallow rooted agricultural crops are suffering from water shortage at the end of the dry season.

The actual evapotranspiration rates derived from *SEBAL* seem quite reasonable. However, more study is needed to verify the energy components determined from remote sensing imagery using *SEBAL* with those measured on the ground with eddy covariance systems and scintillometers. After validation in the field, *SEBAL* holds promise to estimate evapotranspiration rates in the Panama Canal Watershed for a fraction of the costs needed for the installation of a watershed wide network of eddy covariance systems.

### ACKNOWLEDGEMENTS

We appreciate the support for this research received from the Army Research Office, US Yuma Proving Ground Tropic Regions Test Center, New Mexico Tech, and the Universidad Tecnológica de Panama.

### REFERENCES

- Allen, RG, Bastiaanssen, WBM, Tasumi, M, and Morse, A., 2001, Evapotranspiration on the watershed scale using the *SEBAL* model and LandSat Images: Paper #01-2224, ASAE, Ann. Int. Meeting, Sacramento, CA.
- Bastiaanssen, WGM, 1995, Regionalization of surface flux densities and moisture indicators in composite terrain: Ph.D. Thesis, Wageningen Agricultural Univ. (also appeared as Report 109, DLO Winand Staring Centre), Wageningen, The Netherlands: 273p.

- Bastiaanssen, WGM, Menenti, M, Feddes, RA, and Holtslag, AAM, 1998a, A remote sensing surface energy balance algorithm for land (*SEBAL*), Part 1, Formulation: *Jour. Hydrol.*, 212-213:198–212.
- Bastiaanssen, WGM, Pelgrum, H, Wang, J, Ma, Y, Moreno, JF, Roerink, GJ, Roebeling, RA, and van der Wal, T., 1998b, A remote sensing surface energy balance algorithm for land (*SEBAL*), Part 2, Validation: *Jour. Hydrol.*, 212–213:213–229.
- Bastiaanssen, WGM and Bos, MG, 1999, Irrigation performance indicators based on remotely sensed data: a review of literature: *Irrigat. Drain. Sys.*, 13:291-311.
- Bastiaanssen, WGM, Ahmad, MD, and Chemin, Y, 2002, Satellite surveillance of evaporative depletion across the Indus Basin: *Water Resour. Res.*, 38: 1273-1281.
- Bastiaanssen, WGM, 2000, *SEBAL* -based sensible and latent heat fluxes in the irrigated Gediz Basin, Turkey: *Jour. Hydrol.*, 229: 87-100.
- Brutsaert, W, 1982, *Evaporation into the Atmosphere*: Reidel Pub., Dordrecht, The Netherlands.
- Brutsaert, W, Hsu, AY, and Schmugge, TJ, 1993,. Parameterization of surface heat fluxes above a forest with satellite thermal sensing and boundary layer soundings: *Jour. Appl. Meteorol.*, 32: 909–917.
- Camillo, PJ, Gurney, RJ, and Schmugge, TJ, 1983m, A soil and atmospheric boundary layer model for evapotranspiration and soil moisture studies: *Water Resour. Res.*, 19: 371–380.
- Campbell, GS and Norman, JM, 1998, *An Introduction to Environmental Biophysics*: Springer-Verlag, New York, NY.
- Carlson, TN, Gillies, RR, and Perry, EM, 1994, A method to make use of thermal infrared temperature and NDVI measurements to infer soil water content and fractional vegetation cover: *Remote Sens. Rev.* 52: 45–59.
- Farah, HO, 2001, Estimation of Regional Evaporation Under Different Weather Conditions from Satellite and Meteorological Data. A Case Study in the Naivasha Basin, Kenya: Doctoral Thesis Wageningen Univ.
- Franks, SW and Beven, KJ, 1997, Estimation of evapotranspiration at the landscape scale: a fuzzy disaggregation approach: *Water Resour. Res.*, 33: 2929–2938.
- Georgakakos, KP and Sperflage, JA, 2005, Operational Rainfall and Flow Forecasting for the Panama Canal Watershed: in *The Rio Chagres: A Multidisciplinary Perspective of a Tropical River Basin* (RS Harmon, ed.), Kluwer Acad./Plenum Pub., New York, NY: 323-333.
- Hall, FG, Huemmrich, KF, Goetz, SJ, Sellers, PJ, and Nickeson, JE. 1992, Satellite remote sensing of the surface energy balance: success, failures and unresolved issues in FIFE: *Jour. Geophys. Res.*, 97: 19,061–19,090.
- Hendrickx, JMH, Hong, S-H, Miller, T, Small, E, Neville, P, Cleverly, J, and Bastiaanssen, WGM, 2002, Actual ET rates derived by *SEBAL* in the Middle Rio Grande Valley: (abs) Am. Geophys. Union Annual Meeting, San Francisco.
- Huette, AR, 1988, Soil-adjusted vegetation index (SAVI): *Remote Sens. Env.* 25: 89-105.
- Iqbal, M, 1983, *An Introduction to Solar Radiation*: Academic Press, Toronto, Canada.
- Jackson, RD, Reginato, RJ, and Idso, SB, 1977, Wheat canopy temperature: a practical tool for evaluating water requirements: *Water Resour. Res.*, 13: 651-656.
- Kalman, JD and Jupp, DLB, 1990, Estimating evaporation from pasture using infrared thermography: evaluation of a one-layer resistance model: *Agr. Forest Meteorol.*, 51: 223–246.
- Kustas, WP and Norman, JM, 1996, Use of remote sensing for evapotranspiration monitoring over land surfaces: *Hydrol. Sci. Jour.*, 41: 495–515.



- Nieuwenhuis, GJ., Schmidt, EA, and Thunnissen, HAM, 1985, Estimation of regional evapotranspiration of arable crops from thermal infrared images: *Int. Jour. Remote Sens.*, 6: 1319–1334.
- Rosema, A, 1990, Comparison of meteosat-based rainfall and evapotranspiration mapping of Sahel region: *Remote Sens. Env.*, 46: 27–44.
- Seguin, B and Itier, B, 1983, Using midday surface temperature to estimate daily evaporation from satellite thermal IR data: *Int. Jour. Remote Sens.*, 4: 371–383.
- Sellers, PJ, Heiser, MD, and Hall, FG, 1992, Relationship between surface conductance and spectral vegetation indices at intermediate ( $100\text{m}^2$ – $15\text{km}^2$ ) length scales: *Jour. Geophys. Res.* 97: 19033–19059.
- Wang, J, Bastiaanssen, WGM, Ma, Y, and Pelgrum, H, 1998, Aggregation of land surface parameters in the oasis-desert systems of Northwest China: *Hydrol. Proc.*, 12: 2133–2147.